Received: 26 October 2021 | Revised: 4 March 2022 | Accepted: 21 March 2022

DOI: 10.1002/eap.2655

ARTICLE

ECOLOGICAL APPLICATIONS
ECOLOGICAL SOCIETY OF AMERICA

Beyond carbon flux partitioning: Carbon allocation and nonstructural carbon dynamics inferred from continuous fluxes

Guofang Miao[1,2,3] | **Asko Noormets**[3,4] | **Michael Gavazzi**[5] | **Bhaskar Mitra**[6] | **Jean-Christophe Domec**[7,8] | **Ge Sun**[5] | **Steve McNulty**[5] | **John S. King**[3]

[1]Fujian Provincial Key Laboratory for Subtropical Resources and Environment, Fujian Normal University, Fuzhou, Fujian Province, China

[2]School of Geographical Sciences, Fujian Normal University, Fuzhou, Fujian Province, China

[3]Department of Forestry and Environmental Resources, North Carolina State University, Raleigh, North Carolina, USA

[4]Department of Ecosystem Science and Management, Texas A&M University, College Station, Texas, USA

[5]Eastern Forest Environmental Threat Assessment Center, Southern Research Station, USDA Forest Service, Research Triangle Park, North Carolina, USA

[6]School of Informatics, Computing and Cyber Systems, Northern Arizona University, Flagstaff, Arizona, USA

[7]Bordeaux Sciences AGRO, UMR1391 ISPA INRA, Gradignan Cedex, France

[8]Nicholas School of the Environment, Duke University, Durham, North Carolina, USA

Correspondence
Guofang Miao
Email: guofang.miao@gmail.com

Funding information
Ameriflux Management Project, Grant/Award Number: M1800063; Eastern Forest Environmental Threat Assessment Center, Grant/Award Numbers: 08-JV-11330147-038, 13-JV-11330110-081; NIFA, Grant/Award Number: 2014-67003-22068; Office of Science; Southeast Climate Science Center; U.S. Department of Energy; United States Geological Survey, Grant/Award Number: G10AC00624; US DOE Terrestrial Ecosystems Program, Grant/Award Number: DE-SC0006700; USDA; USDA Forest Service; USDA McIntire-Stennis Cooperative Forestry Program, Grant/Award Number: 121209; Weyerhaeuser Corporation

Handling Editor: Yude Pan

Abstract

Carbon (C) allocation and nonstructural carbon (NSC) dynamics play essential roles in plant growth and survival under stress and disturbance. However, quantitative understanding of these processes remains limited. Here we propose a framework where we connect commonly measured carbon cycle components (eddy covariance fluxes of canopy CO_2 exchange, soil CO_2 efflux, and allometry-based biomass and net primary production) by a simple mass balance model to derive ecosystem-level NSC dynamics (NSC_i), C translocation (dC_i), and the biomass production efficiency (BPE_i) in above- and belowground plant (i = agp and bgp) compartments. We applied this framework to two long-term monitored loblolly pine (*Pinus taeda*) plantations of different ages in North Carolina and characterized the variations of NSC and allocation in years under normal and drought conditions. The results indicated that the young stand did not have net NSC flux at the annual scale, whereas the mature stand stored a near-constant proportion of new assimilates as NSC every year under normal conditions, which was comparable in magnitude to new structural growth. Roots consumed NSC in drought and stored a significant amount of NSC post drought. The above- and belowground dC_i and BPE_i varied more from year to year in the young stand and approached a relatively stable pattern in the mature stand. The belowground BPE_{bgp} differed the most between the young and mature stands and was most responsive to drought.

With the internal C dynamics quantified, this framework may also improve biomass production estimation, which reveals the variations resulting from droughts. Overall, these quantified ecosystem-scale dynamics were consistent with existing evidence from tree-based manipulative experiments and measurements and demonstrated that combining the continuous fluxes as proposed here can provide additional information about plant internal C dynamics. Given that it is based on broadly available flux data, the proposed framework is promising to improve the allocation algorithms in ecosystem C cycle models and offers new insights into observed variability in soil–plant–climate interactions.

KEYWORDS
flux partitioning, mass balance, nonstructural carbon, pine plantation, plant carbon allocation

INTRODUCTION

Terrestrial plant carbon (C) dynamics play an essential role in regulating greenhouse gases and mitigating climate change (Beer et al., 2010; Pugh et al., 2019). The components of C dynamics, which are defined to include C storage, internal C fluxes, and external fluxes between plants and environment in biogeochemical models, interact with each other and respond to environmental changes with different feedbacks (Bonan, 2019). The combined outcomes of these feedbacks are complex under global change, and modeling studies remain poorly constrained (Falkowski et al., 2000; Frank et al., 2010). In contrast to the C storage of structural biomass and external fluxes through photosynthesis and respiration, which have been intensively measured and investigated in recent decades, transitional pools and processes, of which the nonstructural C (NSC) and C allocation to various compartments are the two critical components, remain poorly constrained, and some of the most challenging uncertainties that limit our understanding of plant–environment interactions and the modeling of these processes (Babst et al., 2020; Dietze et al., 2014).

Photosynthetic assimilates are allocated to the production of different tissues and can be stored as NSC along the phloem transport pathway. This dynamic plays a critical role in regulating plant responses under nutrient, water, temperature, light stresses, or other environmental effects and mediating biomass turnover in ecosystems (Cannell & Dewar, 1994; Chapin III et al., 1990; Dietze et al., 2014; Kozlowski, 1992; Martinez-Vilalta et al., 2016). However, the regulatory mechanism is still debated, with various hypotheses proposed to develop models (Franklin et al., 2012; Prescott et al., 2020) of which few have captured the dynamics observed in experimental observations (Merganičová et al., 2019). Possible reasons for this include fundamental misunderstanding of the nature of these processes and the lack of sufficient available observations, especially data collected under natural conditions.

It has long been hypothesized that NSC is stored when assimilate supply exceeds utilization demand and the NSC reserve is remobilized for growth, metabolic, or energy needs when the utilization demand exceeds supply (Cannell & Dewar, 1994). Linking to these theoretical hypotheses, much of our current understanding of NSC dynamics is based on the concentration of different carbohydrate classes, mainly soluble sugars and starch (recently reviewed by He et al., 2020; Li et al., 2018; Martinez-Vilalta et al., 2016) and isotopic composition of NSC compounds (Hartmann & Trumbore, 2016; McCarroll et al., 2017). For example, new growth and respiration are supported primarily by new assimilates (Carbone & Trumbore, 2007), but even decades-old NSC reserves can be utilized (Richardson et al., 2015). However, it remains largely uncertain, due to the limited information delivered by concentration and isotope data, to further quantify the role and dynamic trends of NSC, like the sink-driven regulatory role of NSC (Signori-müller et al., 2021), or the NSC dynamics that might be the balance of active, quasi-active, and passive controls (Dietze et al., 2014). Additionally, these data also lack an informative connection with other components of C dynamics. Our understanding of the pool size and dynamic flux of NSC, especially on the ecosystem scale, remains rudimentary.

It is traditionally suggested that plants adjust their C allocation strategy for obtaining resources that limit growth, for example, increasing C allocation to root biomass under limited nutrients and to leaves under limited light (Chapin III et al., 2011). Alternative hypotheses have been proposed recently whereby C allocation is driven, instead of by limited resources, by surplus C that needs to be discharged

from one organ to others (Prescott et al., 2020). Both mechanisms are proposed in terms of the observed biomass ratios of different organs (Cannell & Dewar, 1994; Poorter et al., 2012), but according to a different hypothesis about whether the organs actively or passively receive the allocated C. One of the fundamental differences could be a stress-driven photosynthetic response or allocation response, and a better understanding of this is particularly important for model development. It remains a formidable challenge to test either hypothesis with only biomass information, so alternative information and approaches are urgently needed to help identify the driving force and dynamics of allocation (Jacquet et al., 2014).

Though quantification of the NSC storage and C allocation dynamics remains limited due to the lack of sufficient available measurements, measurement-based studies that take both into account are even rarer (Klein & Hoch, 2015), and much of the understanding of their combined effects comes from model-based studies (Herrera-Ramírez et al., 2020; Merganičová et al., 2019). Given that NSC and allocation dynamics are tightly connected with photosynthesis, respiration, and structural biomass (McDowell, 2011), the interdependence information that could be contained in fluxes and biomass data has been disproportionately less explored (Granda & Camarero, 2017), and it is only carbon use efficiency that is most frequently derived. Our community has accumulated a large amount of high-frequency flux data over recent decades, for example, photosynthesis and respiration data with eddy covariance technique (e.g., FLUXNET2015, Pastorello et al., 2020) and soil chamber (e.g., COSORE; Bond-Lamberty et al., 2020). Allometry-based biomass data have also been sorted out for various ecosystems (Henry et al., 2013). These networks and data sets have helped improve the modeling of individual processes (Baldocchi, 2008; Carbone & Vargas, 2008) and constrain ecosystem models (Richardson et al., 2010) or bridged the study of C dynamics across various spatiotemporal scales (Zscheischler et al., 2017). Exploiting these data for ecosystem-level information of NSC and allocation dynamics might provide additional data to complement individual tree-based data sets for upscaling the associated processes and help close the mass balance of C fluxes and form a comprehensive view on ecosystem C dynamics (Reichstein et al., 2014).

In this study, we leverage the continuous measurements of eddy covariance and soil chamber fluxes with auxiliary information from allometric measurements and propose a flux measurement–based framework to extract information about internal C flux from the external fluxes and apply it to two different forest ecosystems under a range of environmental conditions. This temporally integrating mass balance carbon allocation (TIMBCA) framework estimates NSC as a mass balance residual and considers productivity and respiration from both above- and belowground compartments. Specifically, our objectives were to (1) quantify the total active NSC at the ecosystem scale that is implicitly involved in above- and belowground C dynamics at specific time scales and, with the NSC flux quantified, (2) estimate C translocation and biomass production (BP) efficiency in above- and belowground compartments. Evaluating the closure of the C balance and extracting the internal C cycling information from external fluxes, we attempt to investigate the dynamics of NSC and allocation related to age and drought and present the potential of the flux-based information for filling gaps in our understanding of C dynamics.

METHODS

Concepts and terminology

The plant C budget of terrestrial ecosystems can be formulated as a mass balance equation (Equation 1), in which gross primary production (GPP) is equal to the sum of net primary production (NPP) and plant respiration (R_p). The ratio of NPP to GPP is typically defined as the C use efficiency (CUE) (Equation 1). NPP can be subdivided into structural BP and nonstructural carbohydrates (Vicca et al., 2012). In practice, this distinction is often not made, and NPP is assumed to equal BP (Clark et al., 2001). In this study, we used BP to specifically define the structural C increment at the time scale of interest and define the difference between BP and NPP as r (Equation 2), which maintains the mass balance at each time step and, theoretically, is the NSC flux. Accordingly, biomass production efficiency (BPE) is the proportion of C sources converted to plant structure, similar to Vicca et al. (2012), but with the NSC flux taken into account (Equation 2), as follows:

$$\begin{cases} \mathrm{GPP} = \mathrm{NPP} + \mathrm{R_p} \\ \mathrm{CUE} = \dfrac{\mathrm{NPP}}{\mathrm{GPP}} \end{cases} \quad (1)$$

$$\begin{cases} \mathrm{GPP} = \mathrm{BP} + r + \mathrm{R_p} \\ \mathrm{BPE} = \dfrac{\mathrm{BP}}{\mathrm{GPP} - r} \end{cases} \quad (2)$$

Flux-measurement-based framework: A conceptual model and regression method

Conceptual model

Equation (2) is a global mass balance equation for a whole plant or an ecosystem. The same relationship would apply individually to above- and belowground sections, except

that, instead of GPP, we would talk of fractions of total assimilates ($fGPP_i$) allocated to each compartment (dC_i, where i = agp and bgp for above- and belowground compartments, respectively; Equation 3):

$$\begin{cases} fGPP_i = dC_i \times GPP = BP_i + r_i + R_i \\ \sum_i dC_i = 1 \end{cases} \quad (3)$$

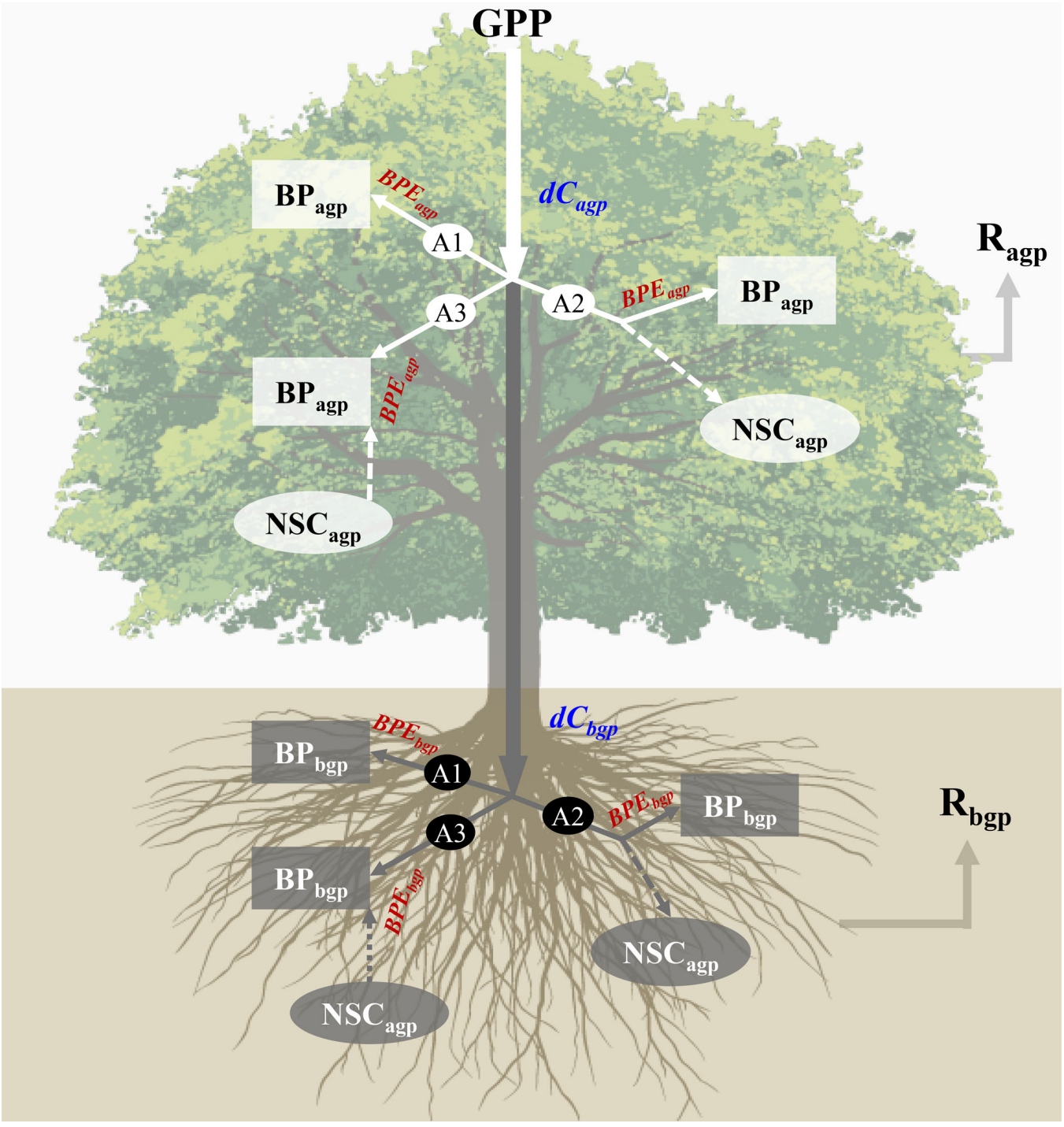

FIGURE 1 Conceptual diagram of carbon (C) translocation (dC_i) of new assimilates (quantified as gross primary production, GPP) to above- and belowground compartments (i = agp and bgp) and C conversion to structural biomass (BP_i) with biomass production efficiencies (BPE_i) (referring to Equations 4–7). Three basic scenarios are included: (A1) the new assimilates ($dC_i \times GPP$) are all used for BP_i; (A2) some new assimilates are stored in local or exported to external compartments as nonstructural C (NSC_i); (A3) stored NSC is activated and used for BP_i. The reality could be different combinations of the three scenarios between above- and belowground compartments.

$fGPP_i$, BP_i, and R_i stand for the new assimilates translocated to, BP, and respiration of the above- or belowground compartments, respectively. The term r_i is the residual of the mass balance, which we hypothesize to represent the active NSC involved in the C cycling of a given compartment. When assimilation and structural BP are in balance, then $r_i = 0$ (Scenario A1 in Figure 1), when some of the assimilated C contributes to the NSC pool, then $r_i > 0$ (Scenario A2), and when growth is in excess of current photosynthesis and draws on stored NSC, then $r_i < 0$ (scenario A3).

The rationale of dividing the whole plant into two pools is based on the availability of continuous measurements of respiratory components—the directly measured ecosystem respiration (R_e), soil respiration (R_s), and aboveground plant respiration (R_{agp}), which is the difference between R_e and R_s (decomposition of coarse woody debris should be included if significant). The belowground plant respiration (R_{bgp}) is derived from R_s partitioning studies. It is important to note that R_{bgp} will affect r_{bgp} estimation, and since most partitioning methods used in the field include mycorrhizas in autotrophic respiration and mycorrhizas also affect carbon allocation to belowground (Hughes et al., 2008), the R_{bgp} generally counts in mycorrhizal respiration and r_{bgp} includes NSC transported to the mycorrhizas.

Of the C used for structural biomass ($dC_i \times GPP - r_i$), only a fraction is turned into BP_i and the rest represents respiratory cost (R_i), i.e., the BPE_i (Equations 4–7). We assumed that if old NSC was mobilized ($r_i < 0$), it was converted with the same efficiency as new assimilates:

$$dC_{agp} \times GPP - r_{agp} = BP_{agp} + R_{agp} \tag{4}$$

$$dC_{bgp} \times GPP - r_{bgp} = BP_{bgp} + R_{bgp} \tag{5}$$

$$BP_{agp} = BPE_{agp} \times \left(dC_{agp} \times GPP - r_{agp}\right) \tag{6}$$

$$BP_{bgp} = BPE_{bgp} \times \left(dC_{bgp} \times GPP - r_{bgp}\right) \tag{7}$$

Combining paired Equations (4) and (6), Equations (5) and (7), we derived Equation (8) and (9):

$$dC_{agp} \times GPP - r_{agp} = BPE_{agp} \times \left(dC_{agp} \times GPP - r_{agp}\right) + R_{agp} \tag{8}$$

$$dC_{bgp} \times GPP - r_{bgp} = BPE_{bgp} \times \left(dC_{bgp} \times GPP - r_{bgp}\right) + R_{bgp} \tag{9}$$

Given that continuous R_{agp}, R_{bgp}, and GPP are usually available, there are five unknowns (dC_{bgp}, BPE_{agp}, BPE_{bgp}, r_{agp}, and r_{bgp}) in the paired equations (8) and (9). We need more information about the linkage among the unknowns to increase the number of equations to solve the five unknowns.

We first introduce the autotrophic fraction of soil respiration α (α = R_{bgp}/R_s), reformulate Equations (8) and (9) to Equations (10) and (11) and then denote the GPP multipliers by c_1 and c_2 and the second terms by t_1 and t_2. Thus, we derive four equations (Equations 12–15). We further define a ratio of aboveground to belowground BP, β (β = BP_{agp}/BP_{bgp}), and then derive the fifth equation from Equations (6) and (7) (Equation 16), as follows:

$$\begin{aligned} R_{agp} &= \left(1 - dC_{bgp}\right) \times \left(1 - BPE_{agp}\right) \times GPP - \left(1 - BPE_{agp}\right) \times r_{agp} \\ &= c_1 \times GPP + t_1 \end{aligned} \tag{10}$$

$$\begin{aligned} R_s &= \frac{dC_{bgp} \times \left(1 - BPE_{bgp}\right)}{\alpha} \times GPP - \frac{1 - BPE_{bgp}}{\alpha} \times r_{bgp} \\ &= c_2 \times GPP + t_2 \end{aligned} \tag{11}$$

$$\left(1 - dC_{bgp}\right) \times \left(1 - BPE_{agp}\right) = c_1 \tag{12}$$

$$dC_{bgp} \times \left(1 - BPE_{bgp}\right) = \alpha c_2 \tag{13}$$

$$-\left(1 - BPE_{agp}\right) \times r_{agp} = t_1 \tag{14}$$

$$-\left(1 - BPE_{bgp}\right) \times r_{bgp} = \alpha t_2 \tag{15}$$

$$\frac{BPE_{agp} \times \left(\left(1 - dC_{bgp}\right) \times GPP - r_{agp}\right)}{BPE_{bgp} \times \left(dC_{bgp} \times GPP - r_{bgp}\right)} = \beta \tag{16}$$

β could be derived from the allometric BP_i estimates, but we do not use the allometric BP directly in our framework because both the temporal and spatial scales differ significantly between the continuous fluxes and manual survey measurements and the uncertainties in absolute values could significantly bias dC_i and r_i.

Flux-regression method

Equations (10) and (11) suggest that if linear relationships exist between R_{agp}, R_s, and GPP, and when expressed on a shorter time scale (e.g., monthly) than the period of interest (e.g., annual), c_1 and c_2 in Equations (10) and (11) are the slopes of the R_i-GPP regression and t_1 and t_2 in Equation (10) and (11) that include r_i are the intercepts. Thus, these five unknown coefficients can be derived from the five equations with field observations. Consistent and well-defined slopes and intercepts

suggest consistent allocation patterns, whereas large standard errors of these metrics and low coefficient of determination (R^2) suggest a variable allocation pattern during the period of interest. The shorter time scale should be selected such that these processes can manifest (which we hypothesize must be aggregated at least to daily level).

We interpret the regression slopes as follows: (i) a significant slope and a high R^2 imply a relatively steady C allocation, quantified by dC_i and BPE_i; (ii) a significant slope but relatively low R^2 value implies that the C allocation may vary within the time scale; the calculated allocation coefficients more likely represent the average status of the C allocation dynamics over the study period; (iii) an insignificant slope indicates that the C allocation varies significantly within the time scale of interest and the conceptual model and the regression approach are not appropriate for this scenario. For the preceding cases (i) and (ii), the intercept of the regression is interpreted as follows: (a) zero intercept indicates no net change in NSC ($r_i = 0$) during the time period of interest (e.g., year), assimilation is in balance with BP (Scenario A1 in Figure 1); (b) negative intercept ($r_i > 0$) indicates surplus assimilates being stored as NSC (Scenario A2); and (c) positive intercept ($r_i < 0$) indicates the use of stored NSC in excess of fresh assimilates (Scenario A3). It is possible for the above- and belowground compartments to exhibit contrasting patterns of NSC involvement (e.g., Figure 2).

We presented here two extreme cases, given the significance of regression slopes and intercepts, to demonstrate the computation of dC_i, BPE_i, and r_i. Both cases assume a significant regression slope. In Case 1, neither above- nor belowground compartments have significant intercepts ($t_1 = 0$, $t_2 = 0$), and in Case 2, both compartments have ($t_1 \neq 0$, $t_2 \neq 0$).

Case 1: No regression intercepts in either compartment

For the case without net NSC flux ($r_i = 0$), β of Equation (16) can be expressed as Equation (17). With the regression slopes c_1 and c_2 and the known α and β (Equations 12 and 13), we can directly solve Equations (12), (13), and (17) and calculate dC_i and BPE_i by Equations (18)–(21), as follows:

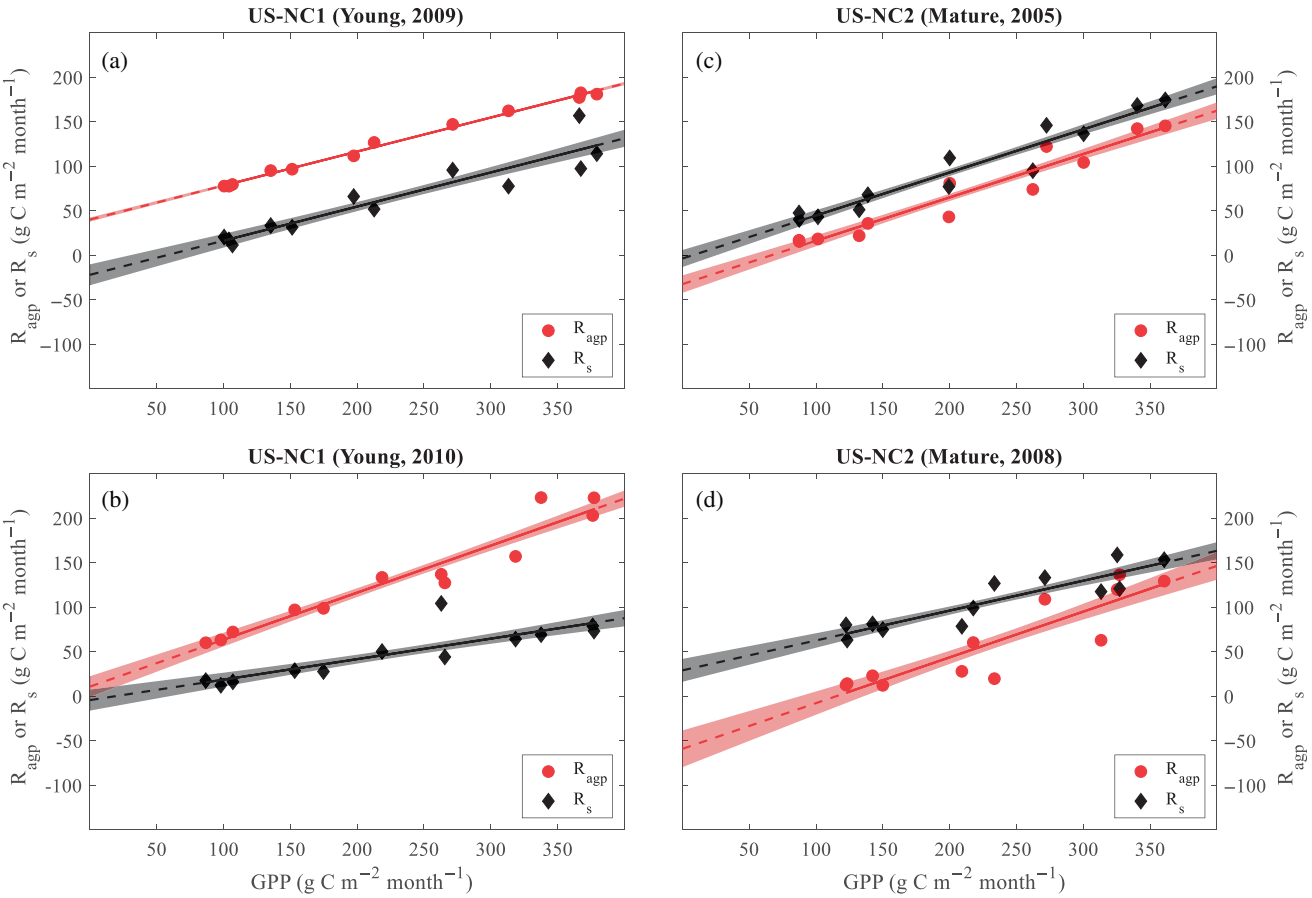

FIGURE 2 Regression between monthly aboveground plant respiration (R_{agp}) and gross primary production (GPP) and between monthly belowground respiration (R_s) and GPP from selected years: (a) 2009 and (b) 2010 at US-NC1 (young plantation) site; (c) 2005 and (d) 2008 at US-NC2 (mature plantation) site. The lines and shaded areas show the fitted values and one SD of the linear regression.

$$\frac{\left(1-\mathrm{dC_{bgp}}\right)\times \mathrm{BPE_{agp}}}{\mathrm{dC_{bgp}}\times \mathrm{BPE_{bgp}}}=\beta \tag{17}$$

$$\mathrm{dC_{bgp}}=\frac{\alpha\beta c_2-c_1+1}{\beta+1} \tag{18}$$

$$\mathrm{BPE_{bgp}}=\frac{1-c_1-\alpha c_2}{\alpha\beta c_2-c_1+1} \tag{19}$$

$$\mathrm{dC_{agp}}=\frac{\beta-\alpha\beta c_2+c_1}{\beta+1} \tag{20}$$

$$\mathrm{BPE_{agp}}=\frac{\beta(1-c_1-\alpha c_2)}{\beta-\alpha\beta c_2+c_1} \tag{21}$$

Case 2: With regression intercepts in both above- and belowground compartments

With NSC involved in both the above- and belowground compartments, β in this case takes its original complex format (Equation 16). With the slopes c_1 and c_2, intercepts t_1 and t_2, known α and β, and GPP, Equations (12)–(16) can be solved for the unknowns, deriving dC_i, BPE_i, and r_i. We used Symbolic Computation of Maple 2017 (Waterloo Maple Inc.) to implement the computation (Appendix S1: Section S1).

We then calculated the whole-plant BPE ($\mathrm{BPE_p}$, Equation 2) based on dC_i, BPE_i, and r_i (Equations 6 and 7). For Case 1, $\mathrm{BPE_p}$ equals the sum of the $\mathrm{dC}_i \times \mathrm{BPE}_i$ in above- and belowground compartments (Equation 22); for Case 2, the calculation of $\mathrm{BPE_p}$ is more complex due to the NSC involvement (Equation 23):

$$\mathrm{BPE_p}=\sum_{i=\mathrm{agp,bgp}}\mathrm{dC}_i\times\mathrm{BPE}_i\ (\text{when } r_i=0) \tag{22}$$

$$\mathrm{BPE_p}=\frac{\sum\limits_{i=\mathrm{agp,bgp}}\mathrm{BPE}_i\times(\mathrm{dC}_i\times\mathrm{GPP}-r_i)}{\mathrm{GPP}-\sum\limits_{i=\mathrm{agp,bgp}}r_i}\ (\text{when } r_i\neq 0) \tag{23}$$

Workflow of data analysis

Data sources

We applied this flux measurement–based framework to two loblolly pine (*Pinus taeda* L.) plantations of different ages to characterize the above- and belowground NSC and allocation dynamics at the ecosystem scale. The two plantations are located in eastern North Carolina in a drained lower coastal plain that favors the growth of plantations and is registered in AmeriFlux as US-NC1 (young plantation, seedlings planted in 2005) and US-NC2 (mature plantation, seedlings planted in 1992) sites (Noormets et al., 2012). Both plantations had simultaneous eddy covariance flux and automated soil CO_2 efflux measurements available for 4 years. Details of the field instrumentation, available flux data sets (daily GPP, R_e, R_s, and R_{agp}), flux uncertainties related to the mass balance assumption, and derivation of input parameters (α and β, Appendix S1: Table S1) are presented in Supporting Information (Appendix S1: Section S2).

The study period spanned from (1) 2009 to 2012 at the US-NC1 site when the trees were 6–9 years old (unclosed canopy with LAI = 3.4–4 $m^2\ m^{-2}$) and (2) 2005 to 2008 at US-NC2 when the trees were 13–16 years old (relatively closed canopy with LAI = 4.4–4.8 $m^2\ m^{-2}$). US-NC1 site was terminated in 2013 and US-NC2 site was thinned in 2009. The two 4-year study periods included a drought from late 2007 through early 2009 with the most severe dry period in 2008, two wet years in 2006 and 2010, and three average-precipitation years in 2005, 2011, and 2012 (Appendix S1: Figure S1; Aguilos et al., 2020).

Regression, computation, and statistical analysis

We explored the NSC dynamics and C allocation on annual and interannual scales by regressing the monthly and annual GPP against monthly and annual R_s and R_{agp}. We first assessed the significance of the regression intercepts and slopes and then computed the NSC and allocation coefficients from the regression slopes or intercepts for the significant cases. Since different combinations of the regression intercepts' significance can be viewed as specific cases of Case 2, we treated all the cases of the two stands from different years as Case 2 and derived the NSC (r_i), allocation coefficients (dC_i and BPE_i), and estimation uncertainties accordingly. Given that β was calculated from annual allometric biomass estimates, we could only carry out the analysis on an annual scale. Ongoing measurements with dendrometer bands will test the resolution of the method on monthly and seasonal scales.

We conducted simple one-way analysis of variance (ANOVA) ($n = 8$) to compare the young and mature stands in the flux regression coefficients (c_1, c_2, t_1, and t_2), r_i, dC_i, and BPE_i. The two stands differed in several dimensions, the chief of which were age, canopy closure, and rooting depth, expected to correspond to different allocation strategies. We assessed the effect of drought on allocation coefficients qualitatively, compared to other years, as the small

sample size limits statistical treatment. Furthermore, continuous R_s data were only available for the older stand in 2008, precluding the site comparison. We also compared the postdrought responses between the two stands in 2009, although the mature stand had incomplete data (January–October 2009) prior to the thinning, to further test the applicability of the framework for quantifying allocation dynamics under different environmental conditions.

All data analyses were done in MATLAB 2018 (MathWorks, Inc.). The NSC and C allocation coefficients are reported as (mean ± SD) to indicate the range of temporal variation. Values for individual years are shown as (mean ± SE) for the estimation uncertainty.

Sensitivity analysis for methodological uncertainties

In this framework, the two input parameters—autotrophic fraction of soil respiration α and above- to belowground biomass increment ratio β—play different roles in determining the dynamics of NSC and allocation coefficients. Determination of these two input parameters carries uncertainties using current methodologies to separate belowground auto- and heterotrophic respiratory components and to quantify above- and belowground biomass. To evaluate the impacts of these uncertainties on the estimation of NSC and allocation coefficients, we first conducted a sensitivity analysis for the mature stand in 2008 to test the robustness of the results for drought effects on the NSC and allocation dynamics by varying either α or β while maintaining the other constant.

Furthermore, we chose 2 years of data from each stand representing a total of four scenarios of environmental conditions and plant responses to conduct sensitivity analyses for a better understanding of the responsive dynamics of NSC and allocation to the variations of α and β. The four scenarios are as follows: (1) mature stand with only aboveground net NSC flux, (2) young stand without net NSC flux, (3) and (4) mature and young stands, respectively, that have net NSC flux in both above- and belowground compartments. We set the ranges of α and β to be 0.1–0.5 (with the interval of 0.05) and 0.5–6.5 (with the interval of 0.5), respectively, based on studies in the literature, representing various ecosystems and covering different environmental conditions, and then calculated r_i, dC_i, BPE_i, and BPE_p. We expected that the derived trends with the wide range would be applicable to a broader context of various ecosystems and conditions and help in further investigations on the interdependence between C allocation and external fluxes.

RESULTS

Linear regression between flux components

Monthly R_{agp} and R_s increased with increasing GPP (see Figure 2 for examples of regression cases (i) and (ii) described in the section *Flux-measurement-based framework: A conceptual model and regression method*). The R^2 was slightly higher for GPP-R_{agp} relationships (range: 0.75–0.99) than for GPP-R_s relationships (range: 0.69–0.95), with all the p values <0.001 (Appendix S1: Table S2). In contrast, the annual fluxes did not exhibit clear relationship patterns between GPP and R_s, R_{agp} (Figure 3; regression case (iii)).

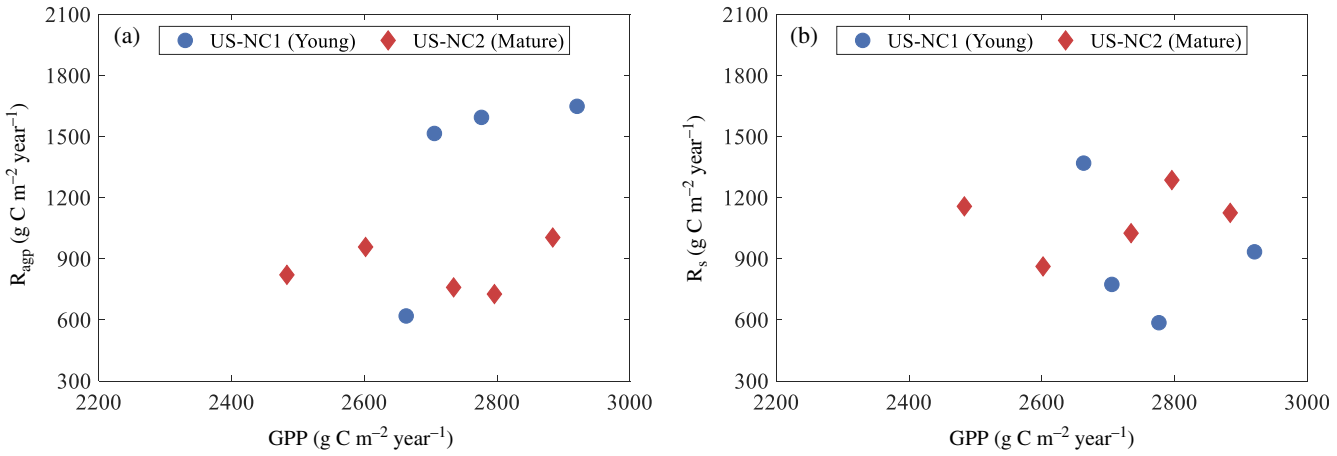

FIGURE 3 Regression between (a) annual total aboveground plant respiration (R_{agp}) and gross primary production (GPP) and (b) annual total soil respiration (R_s) and GPP at US-NC1 (2009–2012) and US-NC2 (2005–2008) sites.

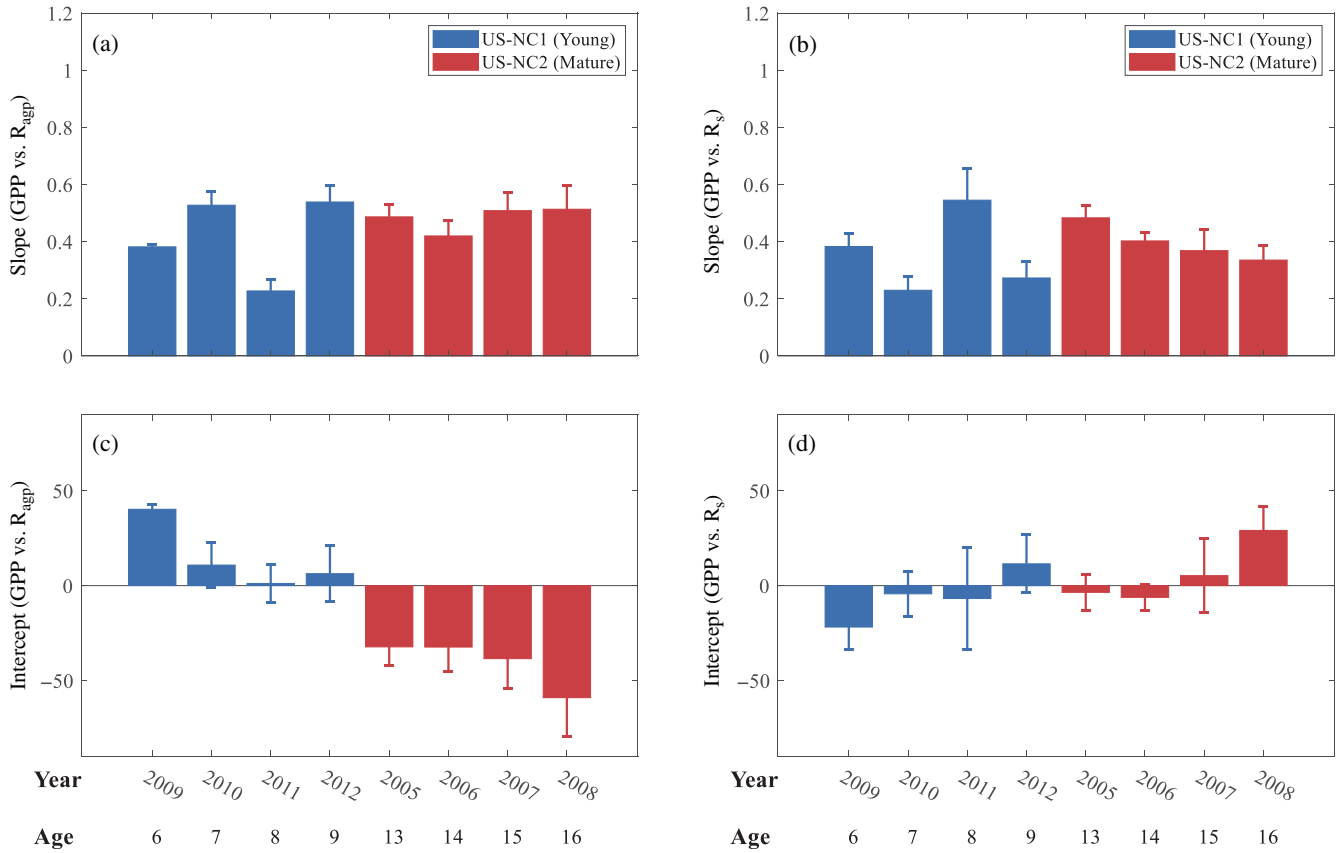

FIGURE 4 Regression coefficients between monthly aboveground respiration (R_{agp}) and gross primary production (GPP) and between monthly soil respiration (R_s) and GPP: (a) GPP-R_{agp} slopes, (b) GPP-R_s slopes, (c) GPP-R_{agp} intercepts, and (d) GPP-R_s intercepts

Over the years, monthly GPP-R_{agp} and GPP-R_s regression slopes (c_1 and c_2 in Equations 10 and 11, respectively) were 0.42 ± 0.15 (mean $\pm$ SD) and 0.36 ± 0.14, respectively, at the young US-NC1 stand and 0.48 ± 0.04 and 0.41 ± 0.06, respectively, at the mature US-NC2 stand. The young stand exhibited higher fluctuations in the slopes of both monthly GPP-R_{agp} and GPP-R_s regressions than the mature stand (Figure 4a, b). The ANOVA did not detect significant differences between the young and mature stands in the mean regression slopes of either above- ($p = 0.44$) or belowground ($p = 0.63$) components.

GPP-R_{agp} and GPP-R_s regression intercepts were both insignificant ($p > 0.35$) at the young stand in all years, except in 2009 ($p < 0.001$ for GPP-R_{agp} and $p = 0.09$ for GPP-R_s, Figure 4c,d), which was the year after the 2008 drought. GPP-R_{agp} regression intercepts were all significant at the mature stand ($p < 0.05$, Figure 4c); however, the intercept of GPP-R_s was only significant in 2008 ($p < 0.05$, Figure 4d), when the drought event lasted throughout the year. The ANOVA indicated that the aboveground regression intercept was significantly different ($p = 0.0022$, Figure 4c) between the young and mature stands. The belowground regression intercept was not significant ($p = 0.32$, Figure 4d), except during the drought in the older stand.

Nonstructural carbon dynamics and allocation coefficients

The r_i, dC_i, and BPE_i calculated from the flux regression slopes and intercepts exhibited more distinct patterns in differences between compartments and between the two stands than the regression coefficients did. In general, the NSC flow, when significant, was higher in the above- than the belowground compartment (Figure 5a). New assimilates supported primarily the aboveground growth, with only 10%–20% of assimilates going to belowground (Figure 5b). The two stands differed significantly in r_{agp} ($p = 0.0078$, Figure 5a) and BPE_{bgp} ($p = 0.00025$, Figure 5c) but insignificantly in the other allocation coefficients (Figure 5).

The young stand did not have a significant net NSC flux during most of the study period in either above- or belowground compartments according to the significance of the regression intercept, except in 2009, the year after

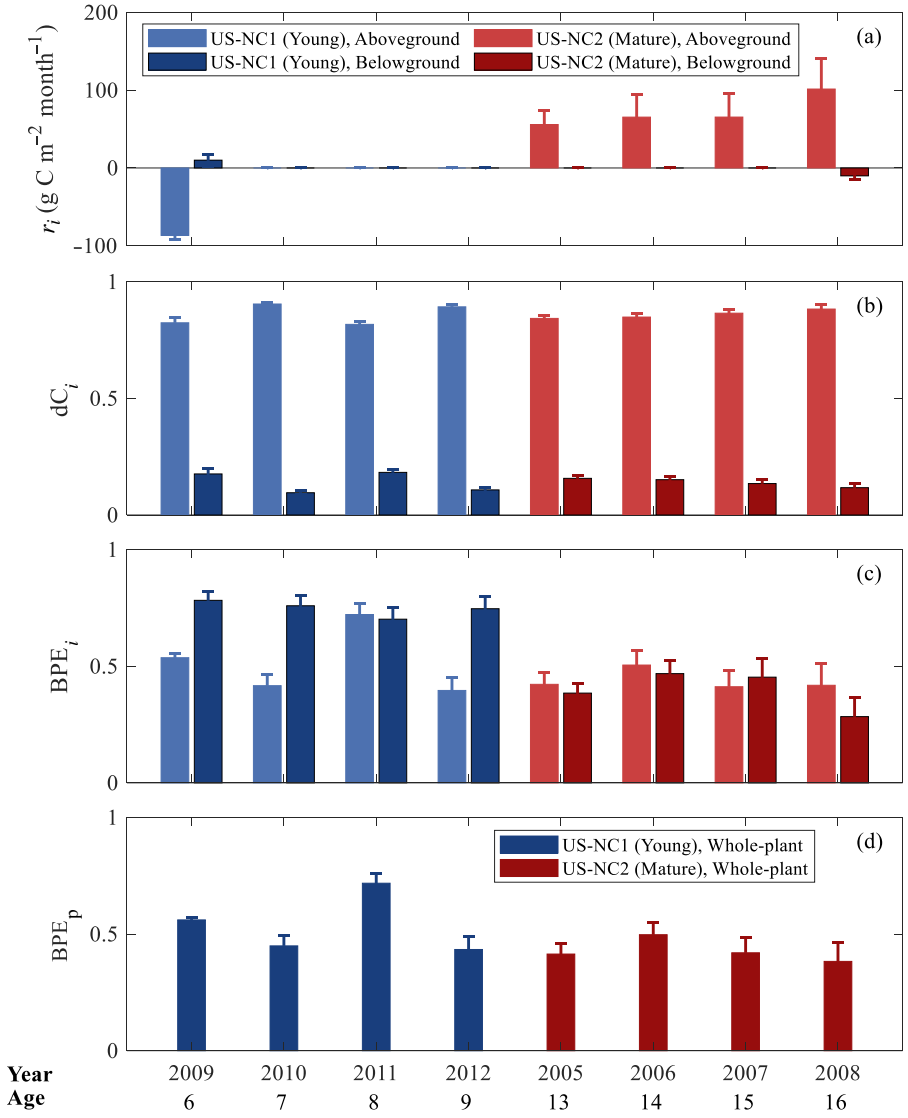

FIGURE 5 Derived above- and belowground (a) nonstructural C storage (r_i), (b) plant C translocation (dC_i), (c) biomass production efficiency for structural biomass (BPE_i), and (d) whole-plant BPE_p.

the drought. The negative r_{agp} ($r_{agp} = -1041.3 \pm 66.2$ g C m^{-2} year^{-1}, mean ± SE) indicates that aboveground growth exceeded the new assimilates translocated to the aboveground compartment, whereas the new assimilates translocated to the belowground compartment were partly used for structural biomass and the rest ($r_{bgp} = 120.4 \pm 92.3$ g C m^{-2} year^{-1}) stored as NSC, exported from roots to rhizosymbionts, or excreted to the soil.

The mature stand allocated a significant fraction of the new assimilates in the aboveground compartment to NSC (r_{agp} of 747.0 ± 66.1 g C m^{-2} year^{-1}) with no significant net NSC flux in the belowground compartment, except in 2008. This stand had a near-constant proportion (27.6 ± 0.9%, mean ± SD) of GPP allocated to be NSC in the three normal years (2005–2007; Appendix S1: Table S3). In the drought year, the aboveground NSC increased up to 44.3% ($r_{agp} = 1218.1 \pm 474.6$ g C m^{-2} year^{-1}, mean ± SE) whereas belowground processes appeared to consume NSC ($r_{bgp} = -121.8 \pm 51.8$ g C m^{-2} year^{-1}, mean ± SE). Despite being small in absolute magnitude, belowground net NSC flux was statistically significant. It is possible that the NSC consumed in the belowground had been imported from the aboveground NSC.

The young stand exhibited somewhat larger fluctuations in dC_i (0.86 ± 0.05 for the aboveground compartment, mean ± SD) than the mature stand (0.86 ± 0.02 for the aboveground plant pool). Across the two stands, the mean dC_{agp} was 0.86 ± 0.03 (mean ± SD) and the mean dC_{bgp} was 0.14 ± 0.03 (Figure 5b).

The absolute values of BPE_{agp} were generally higher in the young stand (0.52 ± 0.15, mean ± SD) than the mature one (0.44 ± 0.04), but due to the large year-to-

year variance in the young stand, the difference was not significantly different ($p = 0.35$). The BPE_{bgp} was relatively stable across the study period and nearly twofold greater in the young (0.75 ± 0.03) than the mature stand (0.44 ± 0.04 excluding the data in 2008, which was 0.28).

Because BPE_p is determined jointly by dC_i, BPE_i, and r_i, it exhibited the traits of all three variables but was primarily driven by dC_i and BPE_i (Equations 22, 23). As a result, BPE_p showed marginally significant differences between the two stands ($p = 0.16$). The BPE_p averaged 0.54 ± 0.13 (mean $\pm$ SD) in the young stand and 0.43 ± 0.05 in the mature stand over the study period (Figure 5d). Thus, like dC_i and BPE_i, BPE_p exhibited higher interannual variation in the young than mature stand.

Uncertainty and sensitivity of nonstructural carbon and allocation coefficients

The differences in r_i between 2008 and other years (mean of 2005–2007) did not significantly change when α varied (Appendix S1: Figure S3a). It implied that the NSC dynamics was primarily affected by the flux regression coefficients rather than α. Likewise, when β varied, the

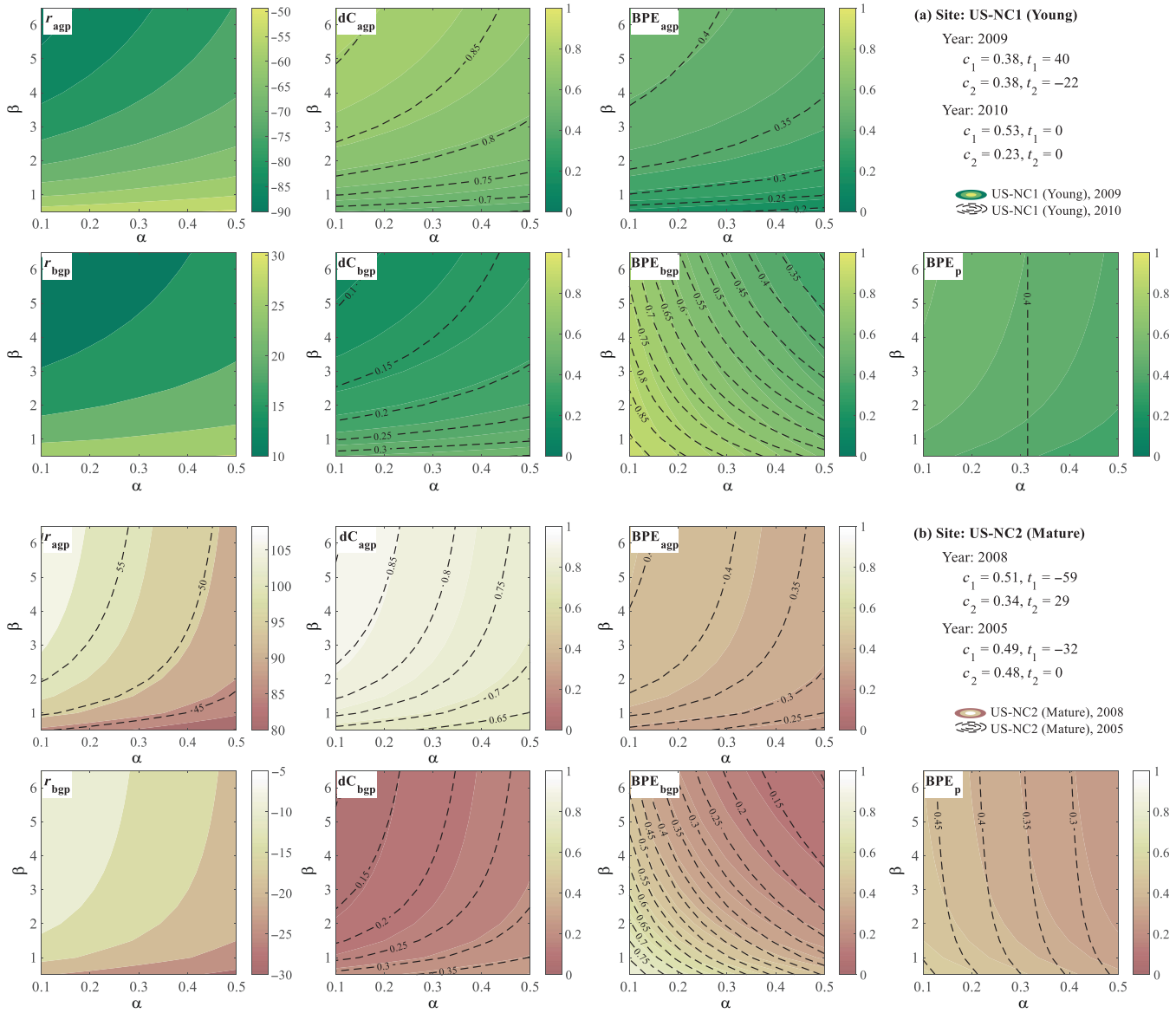

FIGURE 6 Modeled variations of nonstructural C storage (r_i), C translocation (dC_i), biomass production efficiency (BPE_i) of above- (i = agp) and belowground (i = bgp) compartments, and whole-plant BPE_p with the varying α and β in selected years: (a) 2009 and 2010 at US-NC1 (young plantation) site and (b) 2005 and 2008 at US-NC2 (mature plantation) site.

trend of r_i maintained (Appendix S1: Figure S4a). The belowground allocation coefficients, dC_{bgp} and BPE_{bgp}, in contrast, were significantly affected by α and β (Appendix S1: Figures S3b, S3c, S4b, and S4c), which was expected since α is determined by the belowground plant respiration and β by the belowground BP. Despite the great differences in the absolute value, the pattern of most cases remained consistent with the original result, except $\alpha = 0.1$ or $\beta = 1$, when the fractions of belowground plant respiration or BP were assumed to be extremely low.

In the meantime, the sensitivity analysis with varying α and β combined (Figure 6) showed that dC_i and BPE_i, which are decomposed components of BPE_p, had similar responsive patterns to the changes of α and β regardless of whether this involved different years of a given stand (filled contour vs. dashed lines in Figure 6a,b) or the stands (Figure 6a vs. 6b), although the absolute values differed. In contrast, the sensitivity of BPE_p to α and β showed more significant differences between years or stands and, for some scenarios, even exhibited an opposite trend (e.g., young stand in 2009 vs. mature stand in 2008). Of the four coefficients, the absolute value of BPE_{bgp} was the most sensitive to the change of either α or β compared to all the other coefficients.

DISCUSSION

We have described a TIMBCA model that uses continuous C flux measurements to infer the NSC (r_i), C translocation (dC_i), and biomass production efficiency (BPE_i) in above- and belowground compartments and their variation on an interannual scale. We applied this framework to characterize the interannual NSC dynamics and C allocation in two pine plantations. Here we compared the stand-scale patterns with tree-scale patterns reported in previous studies and discussed the consistency and gaps. Results demonstrated the framework's potential as an alternative approach to fill the knowledge gaps in the NSC and C allocation research. We will also discuss the potential uncertainties in the model framework and the limitations of current field measurements.

Dynamics of ecosystem-scale nonstructural carbon

The estimated NSC dynamics in our study suggested that the young stand generally had zero net NSC flux on an annual scale during the normal-precipitation years, whereas the mature stand consistently contributed to the NSC pool each year (Figure 5a). The trend was consistent across years under normal conditions at each stand, and these differences are consistent with earlier reports of mature trees having a larger reservoir of NSC than young trees (Niinemets, 2010; Sala et al., 2012). Our NSC estimation also suggested that the mature stand allocated a near-constant proportion of GPP to NSC under nonstressed conditions.

These consistent stand differences across years provided insights into whether the NSC storage was a priority over growth demand or vice versa (Hartmann et al., 2020; Hartmann & Trumbore, 2016; Sala et al., 2012; Wiley & Helliker, 2012). It is possible that NSC storage is an active choice under nonstressed conditions by mature pine trees and at least at the same priority level as the growth demand on an annual scale. In other words, when trees mature, storing NSC becomes the preferred strategy. Alternatively, the recent "surplus carbon" hypothesis proposed by Prescott et al. (2020) can interpret these stand differences in another view. If new growth is limited by a suboptimal nutrient or water supply, which is more likely to occur in mature stands, extra assimilates would be directed to storage or secondary metabolites. In contrast, the young stand did not have the surplus carbon and as a result had zero net NSC as the small trees had smaller leaf areas and had not yet exhausted the available nutrient supply.

Allocation to NSC increased in the aboveground compartment of the older stand during the drought year (2008), consistent with the observation that drought affects growth more than photosynthesis (He et al., 2020; Li et al., 2018; McDowell, 2011). The attribution of the opposite above-/belowground NSC patterns during the drought and postdrought years to physiological changes is challenging because the 2009 data from the mature stand are incomplete, but the available data at both stands point to the use of NSC. The drought year had a negative r_{bgp}, referring to the consumption of stored NSC in the roots, and the postdrought year had a positive r_{bgp}, referring to the new NSC storage or exporting NSC to rhizosymbionts or excretion to the soil (Figure 5a). It was unfortunate that we could not compare the drought pattern between the two stands, but their postdrought pattern was consistent (Appendix S1: Table S2). While the physiological mechanism behind the consumption/storage of NSC remains to be elucidated, these patterns are consistent with the reports of increases in *root carbohydrate reserve* with drought (Anderegg et al., 2012; Galvez et al., 2011) and the increases in microbial activities following drought (Joseph et al., 2020). A recent study suggested a similar pattern in NSC flux throughout the drought and drought release period (Hagedorn et al., 2016), although, unlike in the current

study, GPP and R_s had more significant responses to drought in their manipulative experiments than in our studies.

Dynamics of carbon allocation coefficients and role of belowground coefficients

The TIMBCA framework describes the carbon allocation dynamics through a set of coefficients—the above- and belowground dC_i and BPE_i. Neither dC_{agp} nor dC_{bgp} showed significant differences between stands and among years, suggesting a relatively steady status of assimilate translocation. Although tests with more years of data under various conditions are required, the steady proportion of assimilate translocation might be determined more by long-term or genetic characteristics than environmental conditions (Reichstein et al., 2014). The BPE_{agp} behaved similarly to dC_i, but BPE_{bgp} exhibited strong dynamics that decreased with age and with drought, which is expected to be affected by the increasing α (Appendix S1: Table S1). Increasing α reflects the growing soil colonization by roots with age (McElligott et al., 2016), and/or the stronger drought suppress of microbial respiration than autotrophic respiration (Noormets et al., 2012). These results might also suggest that BPE_{bgp} rather than dC_i mediates ontogenetic changes and environmental responses (Reichstein et al., 2014).

The sensitivity analysis conducted in this study also implicitly supports the different characteristics among dC_{agp}, dCbgp, BPE_{agp}, and BPE_{bgp}, that is, the less sensitive dC_{agp}, dC_{bgp}, and BPE_{agp} but more sensitive BPE_{bgp} (Figure 6). That BPE_{bgp} is the most sensitive among all the coefficients implicitly illustrates the importance of root C dynamics and its regulatory role when an ecosystem responds to changes (Adamczyk et al., 2019; Norby et al., 2004; Phillips et al., 2012). Notably, a recent study also found that root trait responses are more heterogeneous than leaf trait responses (Lozano et al., 2020), implying more sensitive root responses, although different species and traits were studied. It also suggests that BPE_{bgp} could be an informative physiological trait for investigating root characteristics and belowground processes (Bardgett et al., 2014; Ma et al., 2018). In addition, the combination of decreasing BPE_{bgp} and emerging NSC_{bgp} consumption in the drought year might suggest a different strategy of the mature stand from the NSC_{agp} storage and net zero NSC_{bgp} in normal years, which would be a key question for future exploration. The

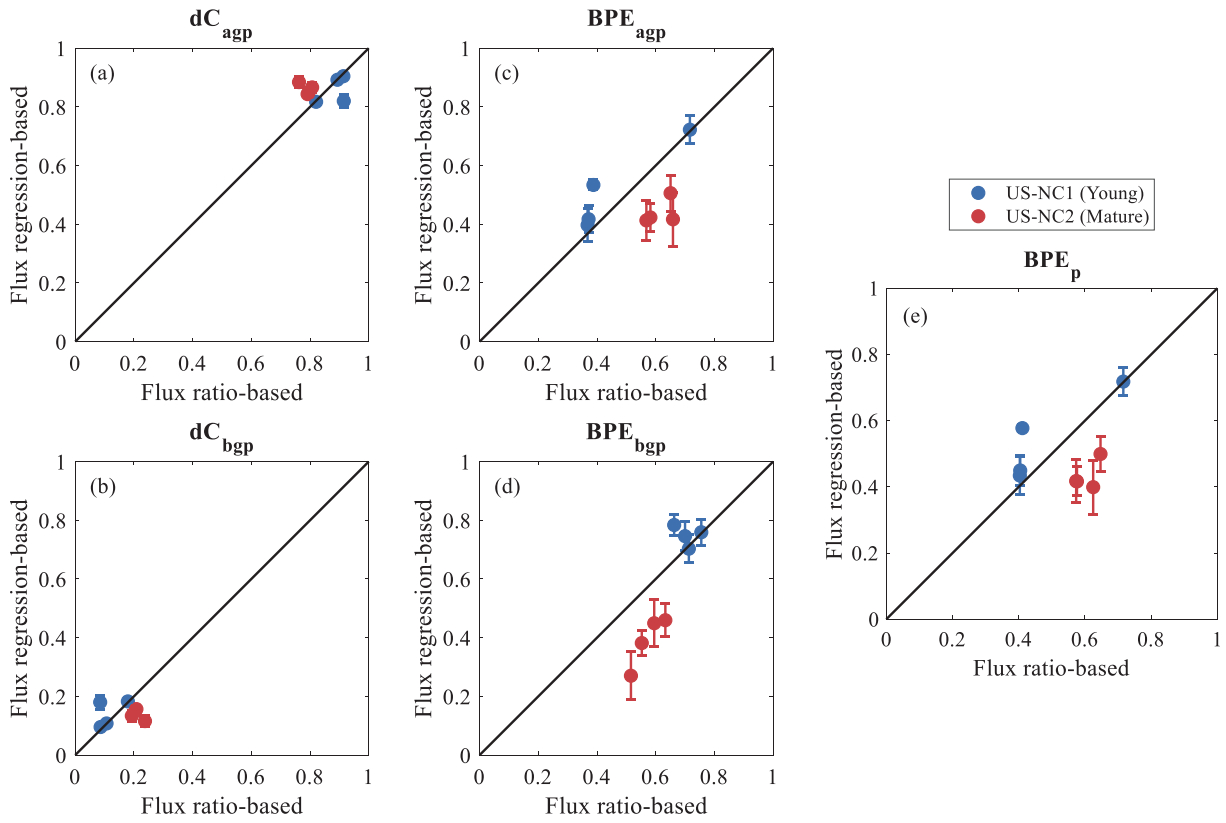

FIGURE 7 Comparison of allocation coefficients derived from flux ratios and flux regression slopes. (a) Carbon translocation to aboveground plant pool, dC_{agp}; (b) carbon translocation to belowground plant pool, dC_{bgp}; (c) aboveground biomass production efficiency, BPE_{agp}; (d) belowground biomass production efficiency, BPE_{bgp}; and (e) whole-plant biomass production efficiency, BPE_p.

added parameter space used in the TIMBCA framework (NSC_i, dC_i, BPE_i, α, and β) extends beyond the current model (GPP, R_p, and CUE), allows us to distinguish different scenarios of interactions, and offers significant promise in terms of explaining the observed patterns in terrestrial C dynamics.

Impact of nonstructural carbon on carbon allocation and biomass production

The two different stands and each stand over different years provided various scenarios of NSC flux. Accordingly, we were able to assess the impact of NSC on allocation and BP, specifically by estimating the deviations between GPP and C consumption, between BP and NPP, and between BPE and CUE, which are all of great importance in C cycle modeling and estimating C turnover rate, but it remains unclear (Collalti & Prentice, 2019). These deviations are best demonstrated by the differences between the ratio of annual R_i/GPP (i.e., without specifying NSC, flux ratio-based) and the slope of R_i and GPP regression (i.e., accounting for NSC, flux regression-based; Appendix S1: Figure S2). In the mature stand in normal years (2005–2007), the annual dC_i and BPE_i (red dots in Figure 7a–d), assuming c_1 and c_2 are equal to the annual flux ratios ($c_1 = R_{agp}/GPP$, $c_2 = R_{bgp}/GPP$), differed by 6.1% to 43.6% compared to the values derived from regression slopes and intercepts; when flux ratio-based BPE_p was calculated as $(1 - R_p/GPP)$, which is also the CUE defined in many previous studies, it overestimated true BPE_p (i.e., the flux regression-based BPE_p in Figure 7e) by 30.1%–39.0%. By contrast, in the young stand without significant NSC flux (2010–2012), the flux ratio-based coefficients were similar to the flux regression-based ones with the much smaller biases (0.1% to 10.9%, blue dots in Figure 7). If we apply the flux ratio-based BPE_p for ecosystems with significant NSC flux to ecosystem models, it is likely that we will overestimate BP for stressed ecosystems and underestimate BP for nonstressed ones.

The biomass production (BP_i) calculated with the flux-based (henceforth referred to as "flux-regression-based"; Equations 6 and 7) and allometric approaches differ in significant ways. The results in Appendix S1: Table S3 are notable in a few aspects, but their full meaning will be elucidated in further studies. First, the sum of BP and NSC in the mature stand are well within the error bounds of the NPP estimates from an earlier analysis (Noormets et al., 2010), and the estimates were similar between the flux- and allometry-based estimates. Remarkably, the NSC flux was roughly equal to BP in the mature stand, and in the drought year NSC was estimated to be twice the BP. Second, the flux-based BP estimates also indicated the decrease in tree growth in the drought year, whereas the allometry-based ones did not. Third, in the young stand, the flux-based BP estimates were double those of allometry-based estimates, raising questions about whether some of the TIMBCA assumptions (especially parameters α and β) may have been in error. We then calculated BP from the sensitivity analysis results to investigate whether α and β might impose large uncertainties on BP estimates. The results show that, even though α and β change in a wide range, the flux-based BP estimates remain much higher than the allometry-based estimates (Appendix S1: Figure S5).

It appears that the allometric method has large uncertainties in estimating short-term BP and biomass change caused by drought due to the measurements and upscaling errors (Jenkins et al., 2003; Vorster et al., 2020). Using repeat allometric measurements for calculating biomass, even along with all necessary corrections for ingrowth and mortality (Clark et al., 2001), should be done with caution because the method is blind to interannual variations and progressive directional changes in allocation, but this limitation is often overlooked. Though the limits of application of the TIMBCA framework remain to be tested, the results reported in this study lend more credibility to these flux-based BP estimates than the allometric ones.

Remaining uncertainties and implications for future studies

Even though our proposed TIMBCA framework can suggest contrasting contributions of NSC to above- and belowground growth, in truth our understanding of NSC deposition and mobilization is very limited. Further details of the internal translocation of NSC and regulation of the use of newly assimilated and old NSC are needed to complete the plant C utilization model. The framework also complements the broad range of C allocation models (e.g., Ogle & Pacala, 2009; and models reviewed by Franklin et al., 2012; Merganičová et al., 2019) by allowing a novel analytical approach since it is entirely based on observational data.

However, several uncertainties remain associated with the assumptions that our framework is based on. The net NSC flux is assumed to be the residual flux among photosynthesis, respiration, and structural biomass, but it remains challenging to specify the source and sink of NSC. We interpreted the NSC flux in this study primarily from the NSC production of new assimilates and the consumption of stored NSC, but conceptually the components of NSC flux could also include transport between above- and belowground

compartments and exudation to soil, for example. The actual NSC source/sink and the components of net flux might differ among various terrestrial ecosystems and await further mechanistic studies. The dynamics of NSC and allocation at finer temporal scales might also help to interpret the possible NSC source and sink.

In the current study, limited by the annual frequency of biometric measurements, we focused on the inter-annual dynamics of allocation metrics using monthly integrated fluxes. The consistency or variability of allocation proportions during a given year is estimated via the SEs of the slopes and intercepts of the models, and it contains uncertainties in that the variations of NSC and allocation at finer temporal scales are averaged. Additionally, the net NSC flux in every year was quantified independently. The year-to-year linkage is yet to be discovered with higher frequency biomass estimates and possibly with the aid of other types of measurements.

Resolving responses at higher frequencies requires biomass estimates at greater frequencies and can be achieved using the recently developed novel automated or remote sensing techniques, for example, dendrometers for stem growth (Zweifel et al., 2021), minirhizotrons for root growth (Defrenne et al., 2021; Yan et al., 2017), and remote sensing for leaf or aboveground biomass (Dana Chadwick & Asner, 2016). Similarly, the temporal dynamics of α should be obtained at a higher frequency as well. Given that above- and belowground growth is known to occur asynchronously (Abramoff & Finzi, 2015), it is reasonable to expect that high-quality and high-resolution biometric data would reveal seasonal or even finer dynamics in allocation patterns. With these components quantified across multiple temporal scales, it is then possible to investigate what drives the dynamic of NSC and allocation and subsequently help differentiate the hierarchy of plant functional processes responding to stresses, both of which are critical components in developing vegetation and ecosystem models (Fatichi et al., 2014).

Overall, the TIMBCA framework offers a method, from a mass balance perspective, of exploiting NSC information in the component fluxes of the ecosystem C cycle and decompose the whole-plant biomass production efficiency (BPE_p) into compartment-level C translocation dC_i and BPE_i. As shown in this study, this flux-based framework characterized the NSC and C allocation dynamics on an annual scale, whose quantified trends were consistent with existing knowledge and evidence and offer promise to improve upon current allocation algorithms that remain poorly constrained (Lawrence et al., 2019). Given that it is based on commonly measured C fluxes, the added complexity and flexibility of the TIMBCA framework and the derived data highlight the potential to fill the knowledge gap of plant internal C dynamics and could open new opportunities for evaluating the potential ranges of ecosystem–climate interactions.

AUTHOR CONTRIBUTIONS

Guofang Miao and Asko Noormets designed the research. Guofang Miao conducted the data analysis. Guofang Miao and Asko Noormets wrote the first draft of the manuscript. Michael Gavazzi maintained the sites and collected field data. All authors provided critical feedback on the draft.

ACKNOWLEDGMENTS

This work was supported, in part, by the US Department of Energy's (DOE) Office of Science through the Ameriflux Management Project (M1800063), USDA Forest Service Eastern Forest Environmental Threat Assessment Center (08-JV-11330147-038, 13-JV-11330110-081), the US DOE Terrestrial Ecosystems Program (11-DE-SC0006700), a Multi-Agency Carbon Cycle Science (A.5) award funded through the USDA National Institute of Food and Agriculture (2014-67003-22068), and a USDA McIntire-Stennis Cooperative Forestry Program (121209). The project was also supported by Grant/Cooperative Agreement Number G10AC00624 from the US Geological Survey as a Southeast Climate Science Center student assistantship to Guofang Miao. Weyerhaeuser Corporation provided site access and generous logistical support.

CONFLICT OF INTEREST

The authors declare no conflict of interest.

DATA AVAILABILITY STATEMENT

The following data sets, available from the AmeriFlux network, were utilized: AmeriFlux US-NC1 data (Noormets, 2018), https://doi.org/10.17190/AMF/1246082; AmeriFlux US-NC2 data (Noormets et al., 2022), https://doi.org/10.17190/AMF/1246083. The COSORE data set (Bond-Lamberty et al., 2020) was also utilized: https://doi.org/10.1111/gcb.15353.

ORCID

Guofang Miao https://orcid.org/0000-0001-5532-932X
Asko Noormets https://orcid.org/0000-0003-2221-2111
Bhaskar Mitra https://orcid.org/0000-0002-6617-0884

REFERENCES

Abramoff, R. Z., and A. C. Finzi. 2015. "Are Above- and below-Ground Phenology in Sync?" *New Phytologist* 205(3): 1054–61. https://doi.org/10.1111/nph.13111.

Adamczyk, B., O. M. Sietiö, P. Straková, J. Prommer, B. Wild, M. Hagner, M. Pihlatie, H. Fritze, A. Richter, and J. Heinonsalo.

2019. "Plant Roots Increase both Decomposition and Stable Organic Matter Formation in Boreal Forest Soil." *Nature Communications* 10(1): 3982. https://doi.org/10.1038/s41467-019-11993-1.

Aguilos, M., B. Mitra, A. Noormets, K. Minick, P. Prajapati, M. Gavazzi, G. Sun, et al. 2020. "Long-Term Carbon Flux and Balance in Managed and Natural Coastal Forested Wetlands of the Southeastern USA." *Agricultural and Forest Meteorology* 288–289: 108022. https://doi.org/10.1016/j.agrformet.2020.108022.

Anderegg, W. R. L., J. A. Berry, D. D. Smith, J. S. Sperry, L. D. L. Anderegg, and C. B. Field. 2012. "The Roles of Hydraulic and Carbon Stress in a Widespread Climate-Induced Forest Die-off." *Proceedings of the National Academy of Sciences of the United States of America* 109(1): 233–7. https://doi.org/10.1073/pnas.1107891109.

Babst, F., A. D. Friend, M. Karamihalaki, J. Wei, G. Von Arx, D. Papale, and R. L. Peters. 2020. "Modeling Ambitions Outpace Observations of Forest Carbon Allocation." *Trends in Plant Science* 26(3): 210–9. https://doi.org/10.1016/j.tplants.2020.10.002.

Baldocchi, D. 2008. "'Breathing' of the Terrestrial Biosphere: Lessons Learned from a Global Network of Carbon Dioxide Flux Measurement Systems." *Australian Journal of Botany* 56(1): 1–26. https://doi.org/10.1071/BT07151.

Bardgett, R. D., L. Mommer, and F. T. De Vries. 2014. "Going Underground: Root Traits as Drivers of Ecosystem Processes." *Trends in Ecology and Evolution* 29(12): 692–9. https://doi.org/10.1016/j.tree.2014.10.006.

Beer, C., M. Reichstein, E. Tomelleri, P. Ciais, M. Jung, N. Carvalhais, C. Rodenbeck, et al. 2010. "Terrestrial Gross Carbon Dioxide Uptake: Global Distribution and Covariation with Climate." *Science* 329(5993): 834–8. https://doi.org/10.1126/science.1184984.

Bonan, G. 2019. *Climate Change and Terrestrial Ecosystem Modeling*. Cambridge: Cambridge University Press. https://doi.org/10.1017/9781107339217.

Bond-Lamberty, B., D. S. Christianson, A. Malhotra, S. C. Pennington, D. Sihi, A. AghaKouchak, H. Anjileli, et al. 2020. "COSORE: A Community Database for Continuous Soil Respiration and Other Soil-Atmosphere Greenhouse Gas Flux Data." *Global Change Biology* 26: 7268–83. https://doi.org/10.1111/gcb.15353.

Cannell, M. G. R., and R. C. Dewar. 1994. "Carbon Allocation in Trees: A Review of Concepts for Modelling." *Advances in Ecological Research* 25: 59–104. https://doi.org/10.1016/S0065-2504(08)60213-5.

Carbone, M. S., and R. Vargas. 2008. "Automated Soil Respiration Measurements: New Information, Opportunities and Challenges." *New Phytologist* 177(2): 295–7. https://doi.org/10.1111/j.1469-8137.2007.02336.x.

Carbone, M. S., and S. E. Trumbore. 2007. "Contribution of New Photosynthetic Assimilates to Respiration by Perennial Grasses and Shrubs: Residence Times and Allocation Patterns." *New Phytologist* 176(1): 124–35. https://doi.org/10.1111/j.1469-8137.2007.02153.x.

Chapin, F. S., III, P. A. Matson, and P. Vitousek. 2011. *Principles of Terrestrial Ecosystem Ecology*. New York, NY: Springer-Verlag.

Chapin, F. S., III, E.-D. S. Stuart, and H. A. Mooney. 1990. "The Ecology and Economics of Storage in Plants." *Annual Review of Ecology and Systematics* 21: 423–47.

Clark, D. A., S. Brown, D. W. Kicklighter, J. Q. Chambers, J. R. Thomlinson, and J. Ni. 2001. "Measuring Net Primary Production in Forests: Concepts and Field Methods." *Ecological Applications* 11(2): 356–70.

Collalti, A., and I. C. Prentice. 2019. "Is NPP Proportional to GPP? Waring's Hypothesis 20 Years on." *Tree Physiology* 39(8): 1473–83. https://doi.org/10.1093/treephys/tpz034.

Dana Chadwick, K., and G. P. Asner. 2016. "Organismic-Scale Remote Sensing of Canopy Foliar Traits in Lowland Tropical Forests." *Remote Sensing* 8(2): 1–16. https://doi.org/10.3390/rs8020087.

Defrenne, C. E., J. Childs, C. W. Fernandez, W. Michael Taggart, R. Nettles, M. F. Allen, P. J. Hanson, and C. M. Iversen. 2021. "High-Resolution Minirhizotrons Advance our Understanding of Root-Fungal Dynamics in an Experimentally Warmed Peatland." *Plants, People, Planet* 3(5): 640–52. https://doi.org/10.1002/ppp3.10172.

Dietze, M. C., A. Sala, M. S. Carbone, C. I. Czimczik, J. A. Mantooth, A. D. Richardson, and R. Vargas. 2014. "Nonstructural Carbon in Woody Plants." *Annual Review of Plant Biology* 65: 667–87. https://doi.org/10.1146/annurev-arplant-050213-040054.

Falkowski, P., R. J. Scholes, E. Boyle, J. Canadell, D. Canfield, J. Elser, N. Gruber, et al. 2000. "The Global Carbon Cycle: A Test of our Knowledge of Earth as a System." *Science* 290(5490): 291–6.

Fatichi, S., S. Leuzinger, and C. Korner. 2014. "Moving beyond Photosynthesis: From Carbon Source to Sink-Driven Vegetation Modeling." *New Phytologist* 201: 1086–95.

Frank, D. C., J. Esper, C. C. Raible, U. Büntgen, V. Trouet, B. Stocker, and F. Joos. 2010. "Ensemble Reconstruction Constraints on the Global Carbon Cycle Sensitivity to Climate." *Nature* 463(7280): 527–30. https://doi.org/10.1038/nature08769.

Franklin, O., J. Johansson, R. C. Dewar, U. Dieckmann, R. E. McMurtrie, A. Ke Br??nnstr??m, and R. Dybzinski. 2012. "Modeling Carbon Allocation in Trees: A Search for Principles." *Tree Physiology* 32(6): 648–66. https://doi.org/10.1093/treephys/tpr138.

Galvez, D. A., S. M. Landhäusser, and M. T. Tyree. 2011. "Root Carbon Reserve Dynamics in Aspen Seedlings: Does Simulated Drought Induce Reserve Limitation?" *Tree Physiology* 31(3): 250–7. https://doi.org/10.1093/treephys/tpr012.

Granda, E., and J. Julio Camarero. 2017. "Drought Reduces Growth and Stimulates Sugar Accumulation: New Evidence of Environmentally Driven Non-Structural Carbohydrate Use." *Tree Physiology* 37(8): 997–1000. https://doi.org/10.1093/treephys/tpx097.

Hagedorn, F., J. Joseph, M. Peter, J. Luster, K. Pritsch, U. Geppert, R. Kerner, et al. 2016. "Recovery of Trees from Drought Depends on Belowground Sink Control." *Nature Plants* 2(8): 1–5. https://doi.org/10.1038/NPLANTS.2016.111.

Hartmann, H., M. Bahn, M. Carbone, and A. D. Richardson. 2020. "Plant Carbon Allocation in a Changing World – Challenges and Progress: Introduction to a Virtual Issue on Carbon Allocation." *New Phytologist* 227: 981–8. https://doi.org/10.1111/nph.16757.

Hartmann, H., and S. Trumbore. 2016. "Understanding the Roles of Nonstructural Carbohydrates in Forest Trees – From What we

Can Measure to What we Want to Know." *New Phytologist* 211: 386–403. https://doi.org/10.1111/nph.13955.

He, W., H. Liu, Y. Qi, F. Liu, and X. Zhu. 2020. "Patterns in Non-structural Carbohydrate Contents at the Tree Organ Level in Response to Drought Duration." *Global Change Biology* 26(6): 3627–38. https://doi.org/10.1111/gcb.15078.

Henry, M., A. Bombelli, C. Trotta, A. Alessandrini, L. Birigazzi, G. Sola, G. Vieilledent, et al. 2013. "GlobAllomeTree: International Platform for Tree Allometric Equations to Support Volume, Biomass and Carbon Assessment." *IForest* 6(6): 326–30. https://doi.org/10.3832/ifor0901-006.

Herrera-Ramírez, D., J. Muhr, H. Hartmann, C. Römermann, S. Trumbore, and C. A. Sierra. 2020. "Probability Distributions of Nonstructural Carbon Ages and Transit Times Provide Insights into Carbon Allocation Dynamics of Mature Trees." *New Phytologist* 226: 1299–311. https://doi.org/10.1111/nph.16461.

Hughes, J. K., A. Hodge, A. H. Fitter, and O. K. Atkin. 2008. "Mycorrhizal Respiration: Implications for Global Scaling Relationships." *Trends in Plant Science* 13(11): 583–8. https://doi.org/10.1016/j.tplants.2008.08.010.

Jacquet, J. S., A. Bosc, A. O'Grady, and H. Jactel. 2014. "Combined Effects of Defoliation and Water Stress on Pine Growth and Non-Structural Carbohydrates." *Tree Physiology* 34(4): 367–76. https://doi.org/10.1093/treephys/tpu018.

Jenkins, J. C., D. C. Chojnacky, L. S. Heath, and R. A. Birdsey. 2003. "National-Scale Biomass Estimators for United States Tree Species." *Forest Science* 49(1): 12–35. https://doi.org/10.1093/forestscience/49.1.12.

Joseph, J., D. Gao, B. Backes, C. Bloch, I. Brunner, and G. Gleixner. 2020. "Rhizosphere Activity in an Old-Growth Forest Reacts Rapidly to Changes in Soil Moisture and Shapes Whole-Tree Carbon Allocation." *Proceedings of the National Academy of Sciences* 117(40): 24885–92. https://doi.org/10.1073/pnas.2014084117.

Klein, T., and G. Hoch. 2015. "Tree Carbon Allocation Dynamics Determined Using a Carbon Mass Balance Approach." *New Phytologist* 205(1): 147–59. https://doi.org/10.1111/nph.12993.

Kozlowski, T. T. 1992. "Carbohydrate Sources and Sinks in Woody Plants." *The Botanical Review* 58(2): 107–222. https://doi.org/10.1007/BF02858600.

Lawrence, D. M., R. A. Fisher, C. D. Koven, K. W. Oleson, S. C. Swenson, G. Bonan, N. Collier, et al. 2019. "The Community Land Model Version 5: Description of New Features, Benchmarking, and Impact of Forcing Uncertainty." *Journal of Advances in Modeling Earth Systems* 11(12): 4245–87. https://doi.org/10.1029/2018MS001583.

Li, W., H. Hartmann, H. D. Adams, H. Zhang, C. Jin, C. Zhao, D. Guan, A. Wang, F. Yuan, and W. Jiabing. 2018. "The Sweet Side of Global Change – Dynamic Responses of Non-Structural Carbohydrates to Drought, Elevated CO2 and Nitrogen Fertilization in Tree Species." *Tree Physiology* 38: 1706–23. https://doi.org/10.1093/treephys/tpy059.

Lozano, Y. M., C. A. Aguilar-Trigueros, I. C. Flaig, and M. C. Rillig. 2020. "Root Trait Responses to Drought Are more Heterogeneous than Leaf Trait Responses." *Functional Ecology* 34(11): 2224–35. https://doi.org/10.1111/1365-2435.13656.

Ma, Z., D. Guo, X. Xingliang, L. Mingzhen, R. D. Bardgett, D. M. Eissenstat, M. Luke McCormack, and L. O. Hedin. 2018. "Evolutionary History Resolves Global Organization of Root Functional Traits." *Nature* 555: 94–7. https://doi.org/10.1038/nature25783.

Martinez-Vilalta, J., A. Sala, D. Asensio, L. Galiano, G. Hoch, S. Palacio, F. I. Piper, and F. Lloret. 2016. "Dynamics of Non- -Structural Carbohydrates in Terrestrial Plants: A Global Synthesis." *Ecological Monographs* 86(4): 495–516.

McCarroll, D., M. Whitney, G. H. F. Young, N. J. Loader, and M. H. Gagen. 2017. "A Simple Stable Carbon Isotope Method for Investigating Changes in the Use of Recent Versus Old Carbon in Oak." *Tree Physiology* 37(8): 1021–7. https://doi.org/10.1093/treephys/tpx030.

McDowell, N. G. 2011. "Mechanisms Linking Drought, Hydraulics, Carbon Metabolism, and Vegetation Mortality." *Plant Physiology* 155(3): 1051–9. https://doi.org/10.1104/pp.110.170704.

McElligott, K. M., J. R. Seiler, and B. D. Strahm. 2016. "Partitioning Soil Respiration across Four Age Classes of Loblolly Pine (*Pinus taeda* L.) on the Virginia Piedmont." *Forest Ecology and Management* 378: 173–80. https://doi.org/10.1016/j.foreco.2016.07.026.

Merganičová, K., J. Merganič, A. Lehtonen, G. Vacchiano, M. Z. O. Sever, A. L. D. Augustynczik, R. Grote, et al. 2019. "Forest Carbon Allocation Modelling under Climate Change." *Tree Physiology* 39(12): 1937–60. https://doi.org/10.1093/treephys/tpz105.

Niinemets, Ü. 2010. "Responses of Forest Trees to Single and Multiple Environmental Stresses from Seedlings to Mature Plants: Past Stress History, Stress Interactions, Tolerance and Acclimation." *Forest Ecology and Management* 260(10): 1623–39. https://doi.org/10.1016/j.foreco.2010.07.054.

Noormets, A. 2018. "AmeriFlux BASE US-NC1 NC_Clearcut, Ver. 3-5." AmeriFlux AMP, dataset. https://doi.org/10.17190/AMF/1246082.

Noormets, A., M. Gavazzi, S. G. McNulty, J.-C. Domec, G. Sun, J. S. King, and J. Chen. 2010. "Response of Carbon Fluxes to Drought in a Coastal Plain Loblolly Pine Forest." *Global Change Biology* 16: 272–87. https://doi.org/10.1111/j.1365-2486.2009.01928.x.

Noormets, A., S. G. Mcnulty, J. C. Domec, M. Gavazzi, G. Sun, and J. S. King. 2012. "The Role of Harvest Residue in Rotation Cycle Carbon Balance in Loblolly Pine Plantations. Respiration Partitioning Approach." *Global Change Biology* 18(10): 3186–201. https://doi.org/10.1111/j.1365-2486.2012.02776.x.

Noormets, A., B. Mitra, G. Sun, G. Miao, J. King, K. Minick, L. Yang, et al. 2022. "AmeriFlux BASE US-NC2 NC_Loblolly Plantation, Ver. 10-5." AmeriFlux AMP, Dataset. https://doi.org/10.17190/AMF/1246083.

Norby, R. J., J. Ledford, C. D. Reilly, N. E. Miller, and E. G. O'Neill. 2004. "Fine-Root Production Dominates Response of a Deciduous Forest to Atmospheric CO2 Enrichment." *Proceedings of the National Academy of Sciences of the United States of America* 101(26): 9689–93. https://doi.org/10.1073/pnas.0403491101.

Ogle, K., and S. W. Pacala. 2009. "A Modeling Framework for Inferring Tree Growth and Allocation from Physiological, Morphological and Allometric Traits." *Tree Physiology* 29(4): 587–605. https://doi.org/10.1093/treephys/tpn051

Pastorello, G., C. Trotta, E. Canfora, H. Chu, D. Christianson, Y. W. Cheah, C. Poindexter, et al. 2020. "The FLUXNET2015 Dataset and the ONEFlux Processing Pipeline for Eddy Covariance

Data." *Scientific Data* 7(1): 225. https://doi.org/10.1038/s41597-020-0534-3.

Phillips, R. P., I. C. Meier, E. S. Bernhardt, S. Grandy, K. Wickings, A. C. Finzi, J. Knops, A. S. Grandy, K. Wickings, and A. C. Finzi. 2012. "Roots and Fungi Accelerate Carbon and Nitrogen Cycling in Forests Exposed to Elevated CO2." *Ecology Letters* 15(9): 1042–9. https://doi.org/10.1111/j.1461-0248.2012.01827.x.

Poorter, H., K. J. Niklas, P. B. Reich, J. Oleksyn, P. Poot, and L. Mommer. 2012. "Biomass Allocation to Leaves, Stems and Roots: Meta-Analyses of Interspecific Variation and Environmental Control." *New Phytologist* 193(1): 30–50. https://doi.org/10.1111/j.1469-8137.2011.03952.x.

Prescott, C. E., S. J. Grayston, H. S. Helmisaari, E. Kaštovská, C. Körner, H. Lambers, I. C. Meier, P. Millard, and I. Ostonen. 2020. "Surplus Carbon Drives Allocation and Plant–Soil Interactions." *Trends in Ecology and Evolution* 35(12): 1110–8. https://doi.org/10.1016/j.tree.2020.08.007.

Pugh, T. A. M., M. Lindeskog, B. Smith, B. Poulter, A. Arneth, V. Haverd, and L. Calle. 2019. "Role of Forest Regrowth in Global Carbon Sink Dynamics." *Proceedings of the National Academy of Sciences of the United States of America* 116(10): 4382–7. https://doi.org/10.1073/pnas.1810512116.

Reichstein, M., M. Bahn, M. D. Mahecha, J. Kattge, and D. D. Baldocchi. 2014. "Linking Plant and Ecosystem Functional Biogeography." *Proceedings of the National Academy of Sciences of the United States of America* 111(38): 13697–702. https://doi.org/10.1073/pnas.1216065111.

Richardson, A. D., M. S. Carbone, B. A. Huggett, M. E. Furze, C. I. Czimczik, J. C. Walker, X. Xiaomei, P. G. Schaberg, and P. Murakami. 2015. "Distribution and Mixing of Old and New Nonstructural Carbon in Two Temperate Trees." *New Phytologist* 206(2): 590–7. https://doi.org/10.1111/nph.13273.

Richardson, A. D., M. Williams, D. Y. Hollinger, D. J. P. Moore, D. B. Dail, E. A. Davidson, N. A. Scott, et al. 2010. "Estimating Parameters of a Forest Ecosystem C Model with Measurements of Stocks and Fluxes as Joint Constraints." *Oecologia* 164(1): 25–40. https://doi.org/10.1007/s00442-010-1628-y.

Sala, A., D. R. Woodruff, and F. C. Meinzer. 2012. "Carbon Dynamics in Trees: Feast or Famine?" *Tree Physiology* 32(6): 764–75. https://doi.org/10.1093/treephys/tpr143.

Signori-müller, C., R. S. Oliveira, F. De Vasconcellos Barros, J. V. Tavares, M. Gilpin, F. C. Diniz, M. J. Marca Zevallos, et al. 2021. "Non-Structural Carbohydrates Mediate Seasonal Water Stress across Amazon Forests." *Nature Communications* 12: 2310. https://doi.org/10.1038/s41467-021-22378-8.

Vicca, S., S. Luyssaert, J. Peñuelas, M. Campioli, F. S. Chapin, P. Ciais, A. Heinemeyer, et al. 2012. "Fertile Forests Produce Biomass more Efficiently." *Ecology Letters* 15(6): 520–6. https://doi.org/10.1111/j.1461-0248.2012.01775.x.

Vorster, A. G., P. H. Evangelista, A. E. L. Stovall, and S. Ex. 2020. "Variability and Uncertainty in Forest Biomass Estimates from the Tree to Landscape Scale: The Role of Allometric Equations." *Carbon Balance and Management* 15(1): 1–20. https://doi.org/10.1186/s13021-020-00143-6.

Wiley, E., and B. Helliker. 2012. "A re-Evaluation of Carbon Storage in Trees Lends Greater Support for Carbon Limitation to Growth." *New Phytologist* 195: 285–9.

Yan, G., F. Chen, X. Zhang, J. Wang, S. Han, Y. Xing, and Q. Wang. 2017. "Spatial and Temporal Effects of Nitrogen Addition on Root Morphology and Growth in a Boreal Forest." *Geoderma* 303: 178–87. https://doi.org/10.1016/j.geoderma.2017.05.030.

Zscheischler, J., M. D. Mahecha, V. Avitabile, L. Calle, N. Carvalhais, P. Ciais, F. Gans, et al. 2017. "Reviews and Syntheses: An Empirical Spatiotemporal Description of the Global Surface-Atmosphere Carbon Fluxes: Opportunities and Data Limitations." *Biogeosciences* 14(15): 3685–703. https://doi.org/10.5194/bg-14-3685-2017.

Zweifel, R., F. Sterck, S. Braun, N. Buchmann, W. Eugster, A. Gessler, M. Häni, et al. 2021. "Why Trees Grow at Night." *New Phytologist* 231(6): 2174–85. https://doi.org/10.1111/nph.17552.

SUPPORTING INFORMATION

Additional supporting information may be found in the online version of the article at the publisher's website.

How to cite this article: Miao, Guofang, Asko Noormets, Michael Gavazzi, Bhaskar Mitra, Jean-Christophe Domec, Ge Sun, Steve McNulty, and John S. King. 2022. "Beyond Carbon Flux Partitioning: Carbon Allocation and Nonstructural Carbon Dynamics Inferred from Continuous Fluxes." *Ecological Applications* e2655. https://doi.org/10.1002/eap.2655